MJFAS MALAYSIAN JOURNAL OF FUNDAMENTAL AND APPLIED SCIENCES
PRINT ISSN: 2289-5981 | ONLINE ISSN: 2289-599X

RESEARCH ARTICLE

The effect of crystallization time and H_2O/CTAB ratio in the synthesis of mesoporous alumina from bauxite residue (red mud)

Omita Riski [a], Didik Prasetyoko [a,*], Dwi Kumala Febrianti [a], Yatim Lailun Ni'mah [a], Vita Nur Iftitahiyah [a], Hartati [b], Imroatul Qoni'ah [a], Eko Santoso [a]

[a] *Department of Chemistry, Faculty of Science, Institut Teknologi Sepuluh Nopember , 60111 Sukolilo, Surabaya, Indonesia*
[b] *Department of Chemistry, Faculty of Science and Technology, Universitas Airlangga, Kampus C UNAIR, Jl. Mulyorejo, Surabaya, 60115, Indonesia*

* *Corresponding author: didikp@chem.its.ac.id*

Article history
Submitted 23 January 2018
Revised 15 March 2018
Accepted 11 July 2018
Published Online 4 February 2019

Graphical abstract

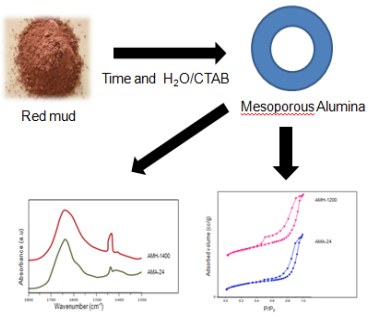

Abstract

Mesoporous alumina has been successfully synthesized from bauxite residues (red mud) as raw material and cetyltrimethylammonium bromide (CTAB) as template at room temperature. The effects of crystallization time and molar ratio of H_2O/CTAB on structural and textural properties of mesoporous alumina were investigated. The synthesized product was characterized by XRD, FTIR, SEM-EDX, TEM, N_2 adsorption-desorption and acidity test using pyridine adsorption. The XRD pattern and SEM micrograph showed that the synthesized product possessed an amorphous phase and irregular shapes. From obtained results, it could be observed that crystallization time and H_2O/CTAB ratio influenced the surface acidity of mesoporous alumina.

Keywords: Red mud, mesoporous, alumina materials, surface acidity

INTRODUCTION

Red mud is a waste material or residue derived from the alumina (Al_2O_3) production from bauxite. The Al_2O_3 production uses Bayer Process in which sodium hydroxide (NaOH) is added to produce Al_2O_3 from bauxite, as well as solid residue called red mud (Kumar, 2015). In average, 1-1.5 tons of red mud may be generated after producing 1 ton of alumina (Brunori *et al.,* 2005). Red mud is comprised from some metal oxides such as iron oxides, silicon oxides and undissolved alumina with a wide range that depended on the ore used (Snars and Gilkes, 2009). The concentration of alumina in red mud is about 25-30% (Liang, 2014). Therefore, red mud can be used as an alumina source to synthesize alumina-based materials.

Alumina has been applied as catalyst, ceramic, catalyst support, conductor and strengthener in composite because of its uniform channels, good thermal conductivity, high Lewis acidity and high specific area (Xia *et al.,* 2003). Red mud from Bintan has been successfully used as raw material to synthesize a mesoporous alumina by adding CTAB as template at room temperature using sol-gel method. Mesoporous alumina from Bintan's red mud confirmed to has a mesoporous structure with BET surface area of 241 m^2/g and pore size of 3.820 nm with ratio CTAB/Al of 0.32 as optimal ratio (Ramdhani *et al.*, 2018).

Sol-gel method is an easy yet cheap method to synthesize mesoporous alumina. Some parameters such as time and water content can be used to optimize the synthesis process. It has been reported that the synthesized product with longer time of aging has bigger particle size (Rousseaux *et al.,* 2002). Water content is proven to give effects on the particle size, crystallinity and specific area of synthesized product (Isley and Penn, 2008).

Here, the synthesis of mesoporous alumina using red mud from Bintan as alumina source and CTAB as template was conducted in room temperature. The effects of crystallization time and molar ratio of H_2O/CTAB on surface acidity of the synthesized product were studied.

EXPERIMENTAL

Materials

The starting materials, the powders of red mud were obtained from Bintan Island of Indonesia, cetyltrimethylammonium bromide (CTAB, Merck, 99%), sodium hydroxide (NaOH, Merck, 99%), hydrochloric acid (HCl, SAP, 37%) and deionized water were used in this study. The chemical composition of Bintan's red mud was shown in Table 1.

Preparation of precursor

The process of extraction and synthesis were adopted from Ramdhani *et al.* (2018). Red mud was leached with HCl 6N solution (solid/liquid ratio 1:5 g/mL) at 90 °C under stirring for 2 h, and then filtered and washed with deionized water. The leachate was collected as aluminum source. Then NaOH 5 N solution was dropped into filtrate under stirring. The $NaAlO_2$ was filtered to separate the precipitate of impurities (Fe^{3+}, Ca^{2+}, etc). HCl 6 N was added to the solution with stirring until the precipitate was completely formed. The

precipitate was used as alumina source in synthesis of mesoporous alumina.

Table 1 Chemical composition analysis by XRF for red mud.

Chemical composition	Mass %
Fe_2O_3	49.87
Al_2O_3	31.39
SiO_2	15.03
TiO_2	1.57
P_2O_5	0.56
K_2O	0.54
CaO	0.15
Cr_2O_3	0.10
V_2O_5	0.08
NiO	0.07
CuO	0.05
ZnO	0.02
Other compound	0.57

Synthesis of mesoporous alumina from red mud

The precipitate from previous steps was mixed with CTAB and water with molar ratio H_2O/CTAB of 600, 800, 1012, 1200 and 1400. The mixture was stirred for 1 h for all samples and then aged for 72 h at room temperature. The final product was recovered by filtration, washed with deionized water and dried at 120 °C for 24 h. The dried product was calcined at 550 °C for 6 h. The effect of crystallization time was studied with molar ratio H_2O/CTAB = 1012. The mixture was stirred for 1 h for all samples and then aged for 3, 12, 24, 48 and 72 h at room temperature. The final product was recovered by filtration, washed with deionized water and dried at 120 °C for 24 h. The dried product was calcined at 550 °C for 6 h. The general method (molar ratio H_2O/CTAB 1012 and aging time 72 h) was adopted from Ramdhani *et al.* (2018). The synthesized sample with variation of crystallization time was labeled as AMA-(crystallization time, h.) for example AMA-24, while sample synthesized with variation of H_2O/CTAB molar ratio was labeled as AMH-(molar ratio of H_2O/CTAB) for example AMH-1200.

Characterization of mesoporous alumina

X-ray powder diffraction patterns of the samples were recorded on a Philips Expert with Cu K_α (40kV, 30 mA) radiation in the range 2θ = 5-50°. The infrared spectra (wavenumber range 400-1400 cm^{-1}) of characteristic vibration bands were monitored by FTIR Shimadzu Instrument Spectrum One 8400S. The specific surface area and pore size distribution were determined from N_2 adsorption-desorption using a Quantachrome Instruments Nova 1200. SEM images and elemental analysis were recorded using Zeiss EVO MA 10 instrument. TEM images were recorded using Hitachi TEM HT7700.

The surface acidity of mesoporous alumina synthesized from red mud was measured by pyridine adsorption using FTIR spectrometer. Calcined samples were pressed into a pellet and then placed in homemade glass transmission cell and outgassed at 400 °C for 4 h under N_2 flow. The pyridine was adsorbed at room temperature for 1 h. Subsequently, the sample was purged under N_2 flow at 150 °C for 3 h. The infrared spectra (range 1300-1800 cm^{-1}) of characteristic vibration band were recorded by FTIR spectrometer.

RESULTS AND DISCUSSION

Synthesis of mesoporous alumina from red mud

Mesoporous alumina has been synthesized from Bintan's red mud with sol-gel mothod. There were some steps involved to prepare the precursor since red mud contained other compounds aside Al_2O_3 such as Fe_2O_3 and SiO_2. The preparation has two steps. The first one was the removal of SiO_2 by adding acid, while the second one was the removal of Fe_2O_3 by adding base. This procedure has been succesfully done by Pan *et al.* (2013) to obtain alumina from coal kaolin and Ramdhani *et al.* (2018) to obtain alumina from Bintan's red mud. Precipitate alumina was formed after adding acid into filtrate from removal Fe_2O_3 process, in which aluminum hydroxide precipitate would form completely in pH ~7 (Pan *et al.,* 2013). This precipitate was used as precursor in synthesis of mesoporous alumina. Fig 1 shows the SEM image and EDX graph for each step in preparation of precursor. As observed from SEM images in Fig 1, all of the residues have an irregular shape and size. According to EDX graph, residue from SiO_2 removal (RSD1) and Fe_2O_3 removal (RSD2) still contained aluminum. This finding was caused by unfinished washing step in each process. Therefore, the residue still contained aluminum. Otherwise, the alumina precipitate (GM-AL) didn't contain any Si or Fe elements which indicated that this process was good enough to obtain alumina from Bintan's red mud.

Alumina salt from previous steps was used as alumina source in synthesis of mesoporous alumina. The mass ratio of CTABr and alumina salt used was 1.57, as reported by Ramdhani *et al.* (2018). The water content inside the alumina salt has been calculated by comparing mass of the salt before and after drying. Alumina salt from the previous steps contained 93.97% of water content that could predict the mass of product to be low. This wet precipitate was added into CTAB solution under strirring for 1 h. The purpose of using wet precipitate was to facilitate the distribution of alumina inside the solution (Ramdhani *et al.,* 2018). The solution was aged for 3, 12, 24, 48 and 72 h. This variation was used to optimize the polimerization process of Al-O-Al so the product would possess stable structure (Moatti *et al.,* 2014). The removal of CTAB was done by calcination at 550 °C for 6 h. There were three steps of CTAB decomposition i.e. ammonia removal at 200-320 °C, structural decomposition of CTAB at 320 °C and removal of the remaining CTAB from alumina structure to form a pore at 395 °C (Liu *et al.,* 2007). Solid product after calcination process was collected. The mass of the product was shown in Table 2. According to Table 2, the mass of product was increased for longer crystallization time. It could be concluded that the effectiveness of polimerization process could be increased for 72 h of crystallization time, as reported by Pan *et al.* (2013) and Ramdhani *et al.* (2018). Sample AMA-72 has the highest mass, due to the synthesis of mesoporous alumina with certain H_2O/CTAB molar ratio at crystallization time for 72 h.

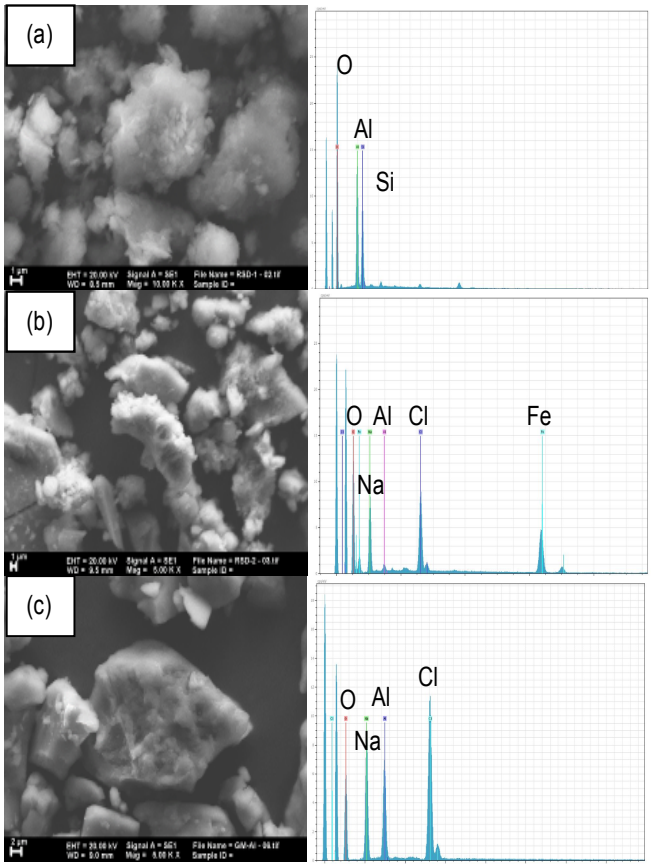

Fig 1. SEM images and EDX graphs of (a) RSD1, (b) RSD2 and (c) GM-AL.

Table 2 Mass of synthesized product with variation of time.

Sample	Mass (g)
AMA-3	0.1810
AMA-12	0.1868
AMA-24	0.1871
AMA-48	0.1932
AMA-72	0.2079

Wang and Ying (1999) have reported that the higher ratio of H_2O could help the hydrolysis process and interfere the particle growth at the same time. Li *et al.* (2004) also confirmed that the higher amount of H_2O in synthesis process, the hydrolysis and polycondensation processes also got faster so the mass of the product could be increased. In this study, the mass of synthesized product was tended to increase with increasing of the molar ratio of H_2O/CTAB. The mass of product with variation of H_2O/CTAB molar ratio was shown in Table 3.

Table 3 Mass of synthesized product with variation of H_2O/CTAB ratio.

Sample	Mass (g)
AMH-600	0.1272
AMH-800	0.1282
AMH-1012	0.1267
AMH-1200	0.1324
AMH-1400	0.1352

Charaterization of mesoporous alumina from red mud

XRD pattern of fresh red mud was shown in Fig. 2. As observed, the Bintan's red mud contained some minerals such as hematite (Fe_2O_3), goethite (FeOOH), gibbsite ($Al(OH)_3$), boehmite (γ-AlO(OH)), anatase (TiO_2) and quartz (SiO_2). This result was confirmed by the elemental analysis of Bintan's red mud with XRF technique (Table 1). The XRD pattern of red mud has a similar pattern as reported by Liang *et al.* (2014), Sushil and Batra (2012), and Ghosh *et al.* (2010).

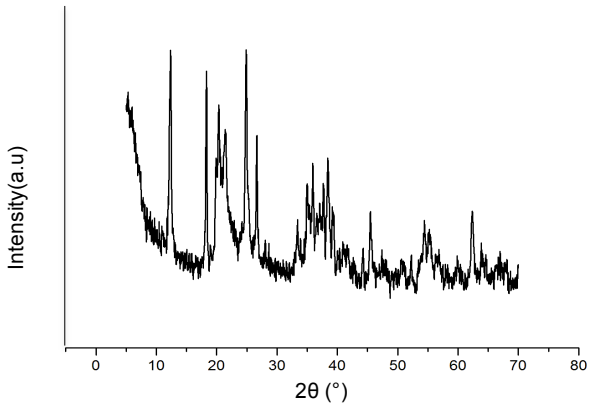

Fig. 2 XRD pattern of red mud.

Fig. 3 and Fig. 4 show the XRD pattern of mesoporous alumina from red mud with variation of crystallization time and H_2O/CTAB molar ratio after calcination at 550 °C for 6 h. There was no characteristic peak detected in XRD pattern for all samples. The absence of the characteristic peak indicated that the material has bimodal porous with amorphous wall (Pan *et al.,* 2013). According to Cheng *et al.* (1995), when synthesis has been done with concentration of CTAB under 40%, the synthesized product has irregular mesopore. Therefore, no peak was detected for all of the samples.

The samples of red mud, as-synthesized alumina, and calcined alumina were investigated by infrared spectroscopy (Fig. 5). Infrared spectra for all calcined samples showed similar spectra, i.e. peak at around 3450 and 1635 cm^{-1} for stretching and bending vibrations of O-H groups, and also at 729 and 590 cm^{-1} for Al-O vibration. Similar infrared spectra were stated by Pan *et al.* (2013). In addition, there was no sharp peak at around 1200-1000 cm^{-1} characteristic for stretching vibration of Si-O (Qoniah *et al.,* 2015), which only appeared in red mud sample. This finding concluded that the solid sample only consisted of alumina. Meanwhile, infrared spectra of as-synthesized sample only showed a peak at around 1400 cm^{-1}, characteristic for bending vibration of $–CH_2$ and $–CH_3$ from cetyltrimethylammonium (Yue *et al.,* 2010). The absence of this peak in all infrared spectra of calcined product indicated that cetyltrimethylammonium was completely removed from the solid product.

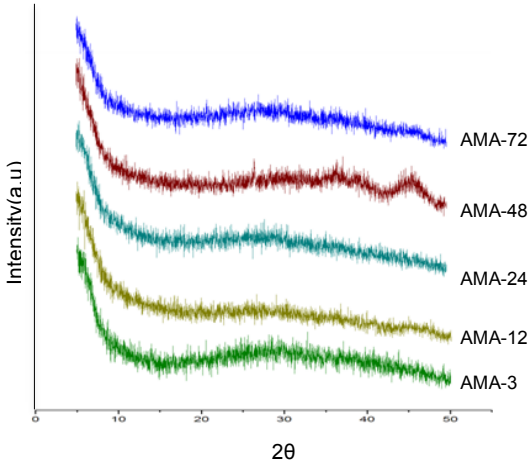

Fig. 3 XRD pattern of mesoporous alumina from red mud with variation of time.

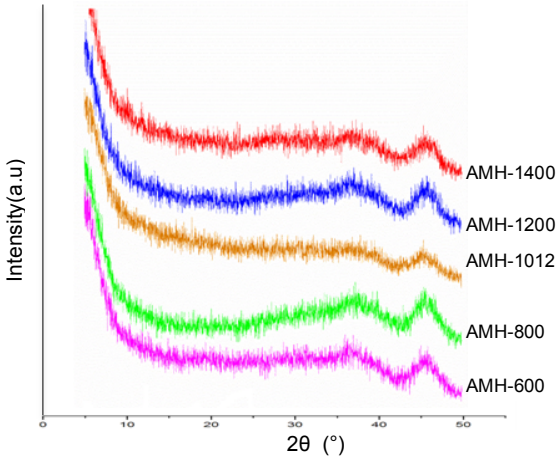

Fig. 4 XRD pattern of mesoporous.

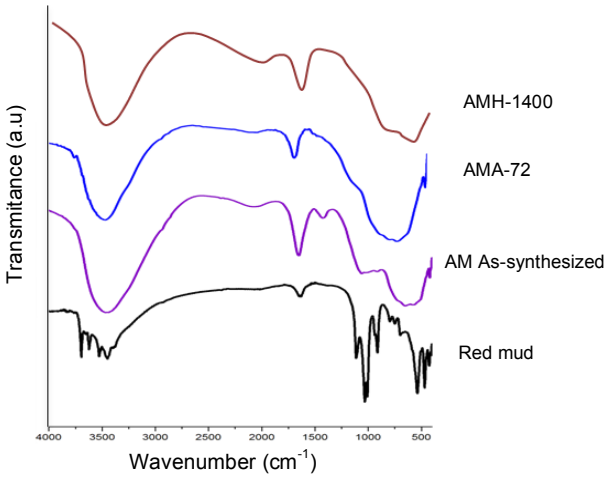

Fig. 5 FTIR Spectra for (a) red mud, (b) As-synthesized mesoporous alumina (AM as-synthesized), (c) AMA-72 and (d) AMH-1400.

The N_2 adsorption-desorption isotherms of the synthesized-alumina from red mud has been carried out to determine the specific surface area, pore size distribution and pore volume of the synthesized materials (Fig. 6). The N_2 adsorption-desorption isotherm for sample AMA-24 showed hysteresis at p/p0 = 0.4-0.9, indicating that the sample has isotherm type IV. According to the isotherm type by IUPAC, it was ~~is~~ confirmed that the synthesized-alumina from red mud contained mesopore. The isotherm adsorption for AMH-1200 also indicated the type IV isotherm based on the presence of H3 hysteresis loop. According to IUPAC classification, the hysteresis loops for AMA-24 and AMH-1200 were apparently composite of H1 and H3 type hysteresis loops, indicating the samples to consist of ~~a~~ plate-like particles and slit-like pores. The type of hysteresis confirmed that the synthesized product has a mesopore and synthesized sample from a clay usually has slit like pores. The pore structure parameters were calculated according to the mathematical models from the N_2 adsorption-desorption. The data were given in Table 4. According to BJH calculation, AMA-24 has 132.122 m^2/g mesoporous surface area with pore size of 3.831 nm and AMH-1200 has 184.474 m^2/g mesoporous surface area with pore size of 3.833 nm. The pore size distribution for AMA-24 and AMH-1200 were shown at Fig. 7. This result showed the similar profiles as reported by Ramdhani *et al.* (2018) with a larger mesoporous surface area. It was interesting to note that AMA-24 and AMH-1200 also have microporous structure since they have pretty high adsorption in p/p0 < 0.3. The BET calculation showed that the microporous surface area for AMA-24 and AMH-1200 were 212.485 m^2/g and 168.311 m^2/g, respectively. The pore volume for AMA-24 and AMH-1200 were 0.426 cc/g and 0.363 cc/g.

Table 4. Pore structure properties of AMA-24 and AMH-1200.

Sample	Mesoporous Surface Area[a] (m^2/g)	Microporous Surface Area[b] (m^2/g)	Pore volume[a] (cc/g)	Pore diameter[a] (nm)
AMA-24	132.122	212.485	0.426	3.831
AMH-1200	184.474	168.311	0.363	3.833

[a] determined by BJH
[b] determined by BET at P/P_0 =0.3

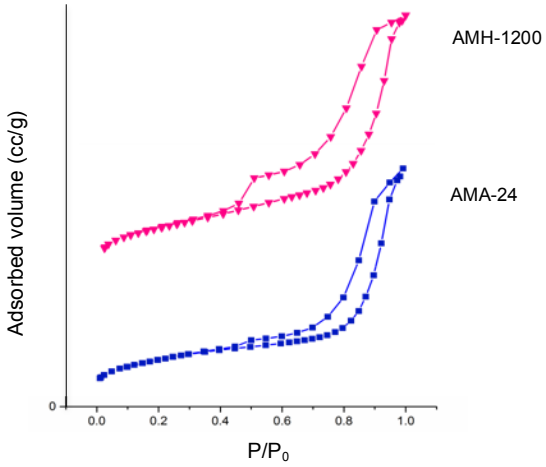

Fig. 6 Nitrogen adsorption-desorption of the samples: (a) AMA-24 and (b) AMH-1200.

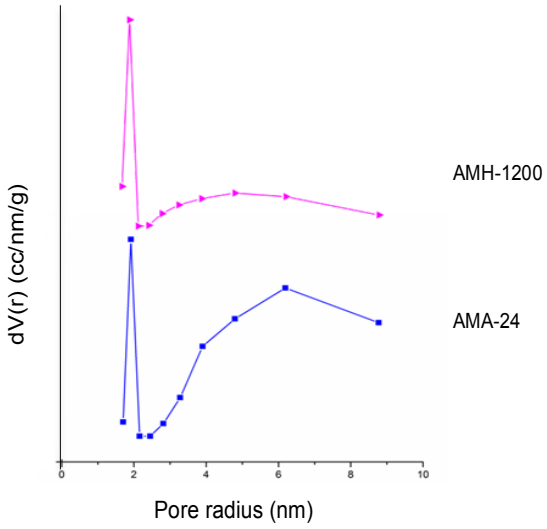

Fig. 7 Pore size distribution of the samples: (a) AMA-24 and (b) AMH-1200.

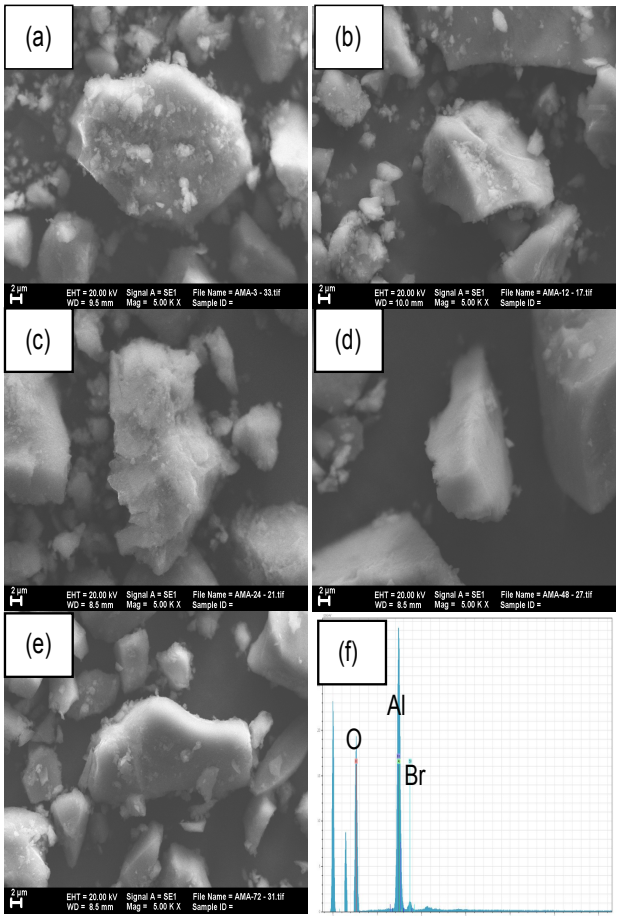

Fig 8. SEM images of (a) AMA-3, (b) AMA-12,(c) AMA-24, (d) AMA-48, (e) AMA-72 and EDX graph of (f) AMA-72.

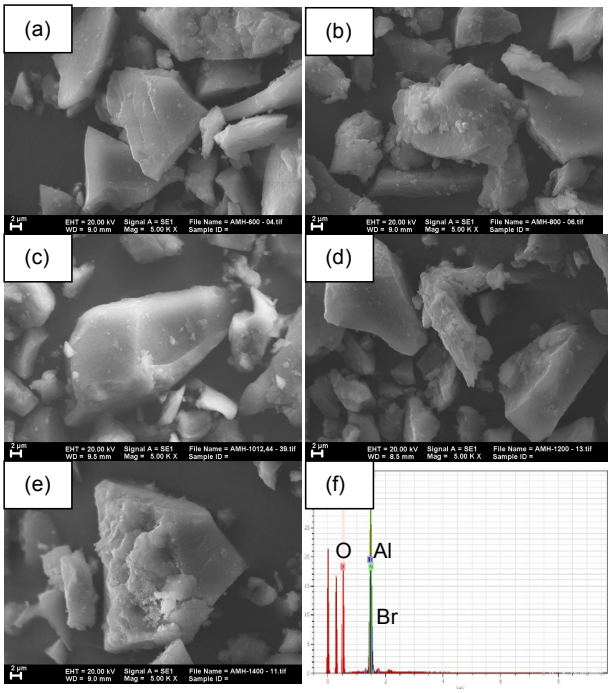

Fig 9. SEM images of (a) AMH-600, (b) AMH-800,(c) AMH-1012, (d) AMH-1200, (e) AMH-1400 and EDX graph of (f) AMH-1200.

The morphology and the elemental analysis of the alumina samples were investigated with SEM-EDX. Morphologies of mesoporous alumina synthesized with variation of crystallization times were shown in Fig 8. The particle size and the formation of mesoporous aggregates were controlled by the reaction condition, such as time, pH and addition of structure directing agent (Petushkov *et al.*, 2011). In this study, the size and shape for all samples were irregular without any particular differences. Meanwhile, morphology of the mesoporous alumina samples synthesized with variation of H_2O/CTAB molar ratios were shown in Fig 9. The obtained result was similar with the result for variation of time. There was no significant difference in the particle size reported by Isley and Penn (2008). It might be caused by the precursors that did not have regular shape to start off. The EDX graph showed peak for bromine for AMA-72 and AMH-1200 samples. The peak for bromine might appear due to unfinished washing procedure, causing ~~so~~ the ions to stay still inside the pore even though calcination was already done.

AMA-72 was investigated with TEM to monitor the morphology of the product as shown in Fig. 10. As observed, AMA-72 has morphology of both wormlike structure (Fig 10 a and b) and thin sheet-like structure (Fig. 10 c and d). In this paper, alumina was synthesized from wet precipitate alumina salt. The water content in the alumina salt was pretty high. Huang *et al.* (2014) reported that the molar ratio of H_2O/Al from the precursor could give an impact to the morphology of the synthesized product. When the water content was increased, the Boehmite plates would get larger and have thin sheet-like structure. It was confirmed that mesoporous alumina from red mud has an excess water content. The wormlike structure from AMA-72 was a characteristic structure from alumina that synthesized by adding surfactant (de Llobet *et al.* 2013). The porous structure of alumina (Fig. 10 (a) and (b)) resulted the formation of irregular pores. Beck *et al.* (1992) reported that molar ratio of surfactant and aluminum < 1 would make hexagonal surfactant system with a regular pore structure. It might be different case since the surfactant used in this study was CTAB. According to Cheng *et al.* (1995), when synthesis has been done with concentration of CTAB < 40%, the synthesized product would exhibit irregular mesopore. Since the mass ratio of CTAB and alumina salt was 1.57, it could be understood that the concentration of CTAB inside the precursor was way below 40% so the product would be expected to possess an irregular pores and shape. These findings also have been reported by Ramdhani *et al.* (2018). The dark part from the AMA-72 showed the close packed of platelets created by random stacking of nano-platelets. The higher water content from precursor, the tighter agglomeration was formed (Huang *et al.*, 2014). We predicted that the slit-like pore that was seen from hysteresis loop (Fig. 6) resulted from this randomly stacked of nano-platelets.

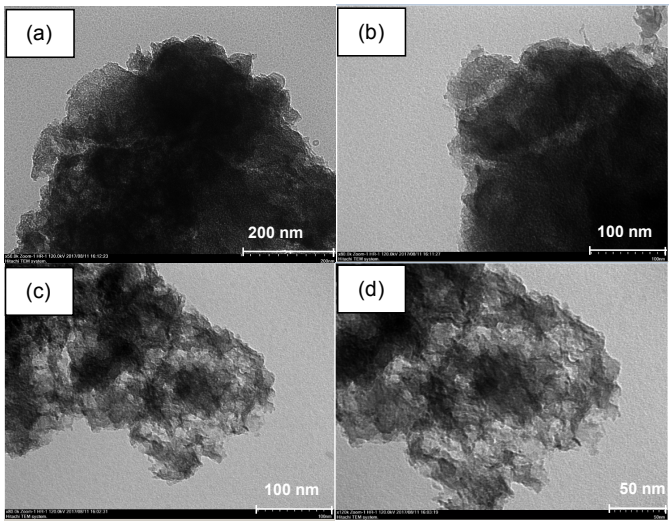

Fig 10. TEM images of AMA-72.

Acidity study

Alumina is one of the solids that has a strong Lewis acid site (Parry, 1963). In this study, the synthesized product was tested using pyridine to identify the surface acidity. After pre-treatment using pyridine sorption, the product was characterized with FTIR and the results were showed in Fig. 11 and Fig. 12.

The infrared spectra showed peak in the range wavenumber of 1447-1440 cm^{-1} for all samples. This peak was identified as characteristic peak for Lewis acid that indicated interaction of pyridine and alumina acid sites (Platon and Thomson, 2003). The peak for Brønsted acid was not found in the wavenumber ~1550 cm^{-1}. This result showed that the product has Lewis acid sites on the surface but not Brønsted acid sites. We concluded that mesoporous alumina synthesized from red mud still has Lewis acid site even though not as strong as mesoporous alumina synthesized from commercial material. Therefore, mesoporous alumina has potential to be catalyst support for increasing surface area and Lewis acid sites of the catalyst.

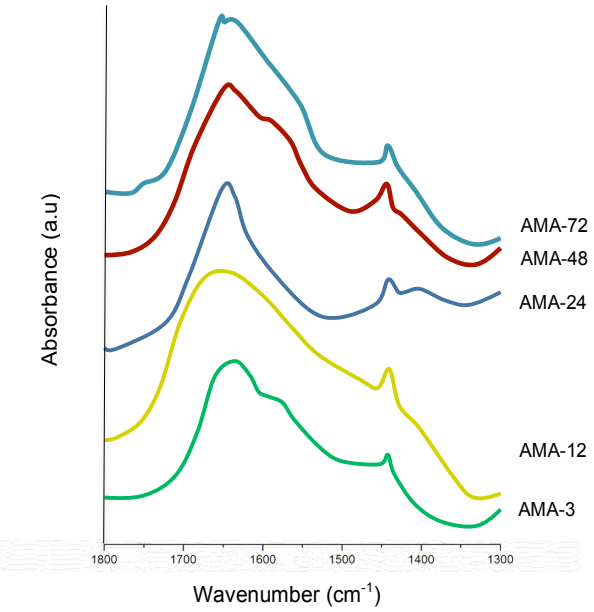

Fig 11. Pyridine-FTIR Spectra of mesoporous alumina from red mud with variation of crystallization time.

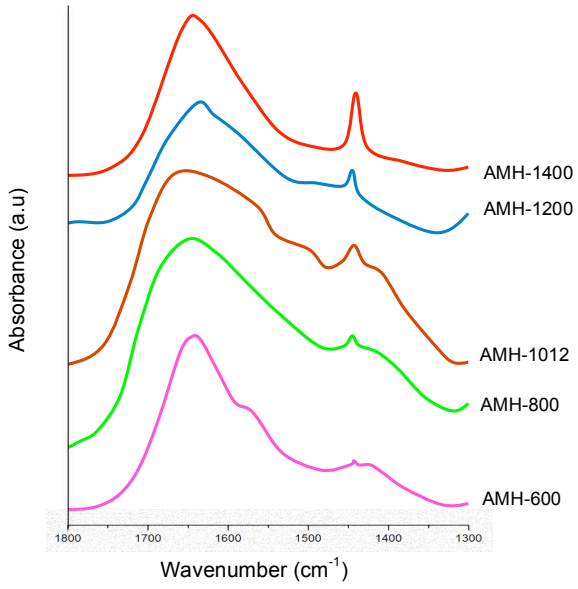

Fig 12. Pyridine-FTIR Spectra of mesoporous alumina from red mud with variation of H_2O/CTAB molar ratio.

CONCLUSION

This study has been proved that bauxite residue (red mud) could be employed as alumina source for synthesis of mesoporous alumina with CTAB as template. The effects of crystallization time and H_2O/CTAB molar ratio were investigated and the obtained results ~~its~~ showed the significant effects on mass of product and acidity of surface. Increasing time of synthesis and H_2O/CTAB molar ratio caused the increase in mass of product and presence of Lewis acid sites on the surface.

ACKNOWLEDGEMENT

The authors gratefully acknowledge the research funding provided by the Ministry of Research, Technology and Higher Education of Indonesia 2017-2018. They would also like to thank the Research Center for Nanoscience and Nanotechnology (RCNN), Institut Teknologi Bandung for TEM measurement.

REFERENCES

Beck, J., Vartuli, J., Roth, W., Leonowicz, M., Kresge, C., Schmitt, K., et al. (1992). A new family of mesoporous molecular sieves prepared with liquid crystal templates. *Journal of American Chemistry Society*, 114, 10834-10843.

Brunori, C., Cremisini, C., Massanisso, P., Pinto, V., & Torricelli, L. (2005). Reuse of a treated red mud bauxite waste: Studies on environmental compatibility. *Journal of Hazardous Materials*, B117, 55–63.

Cheng, C. F., He, H., Zhou, W., & Klinowski, J. (1995). Crystal morphology supports the liquid crystal formation mechanism for the mesoporous molecular sieve MCM-41. *Chemical physics letters*, 244(1), 117-120.

de Llobet, S., Purón, H., Pinilla, J., Moliner, R., Millán, M., & Suelves, I. (2013). Tailored synthesis of organised mesoporous aluminas prepared by non-ionic surfactant templating using a Box-Wilson CCF design. *Microporous and Mesoporous Materials*, 179, 69–77.

Ghosh, I., Guha, S., Balasubramaniam, R., & Kumar, A. V. (2011). Leaching of metals from fresh and sintered red mud. *Journal of Hazardous Materials*, 185, 662–668.

Huang, B., Bartholomew, C. H., & Woodfield, B. F. (2014). Facile synthesis of mesoporous γ-alumina with tunable pore size: The effects of water to aluminum molar ratio in hydrolysis of aluminum alkoxides. *Microporous and Mesoporous Materials*, 183, 37–47.

Isley, S.L., & Penn, R.L. (2008). Titanium dioxide nanoparticle: Effect of sol-gel pH on phase composition, particle size, and particle growth mechanism. *The Journal of Physical Chemistry C,* 112, 4469-4474.

Kumar, S. (2015). The properties and performance of red mud-based geopolymeric Masonry blocks. In Pacheco-Torgal, F., Lourenço, P.B., Labrincha, J.A., Kumar, S., & Chindaprasirt, P. (Ed.) *Eco-Efficient Masonry Bricks and Blocks* (pp. 311-328), Woodhead Publishing, Elsevier.

Li, Y., White, A., & Lim, S. (2004). Low temperature synthesis and microstructural control of titania nano-particles. *Journal of Solid State Chemistry*, 177, 1372-1381.

Liang, W. T., Couperthwaite, S. J., Kaur, G., Yan, C., Johnstone, D. W., & Millar, G. J. (2014). Effect of strong acids on red mud structural and fluoride adsorption properties. *Journal of Colloid and Interface Science*, 423, 158–165.

Liu, Q., Wang, A., Wang, X., & Zhang, T. (2007). Morphologically controlled synthesis of mesoporous alumina. *Microporous and Mesoporous Materials*, 100, 35-44.

Moatti, A., Javadpour, J., Anbia, M., & Badiei, A. (2014). The correlation between aging time and pore characteristics in the synthesis of mesoporous Al_2O_3. *Ceramics International*, 40, 10231–10236.

Pan, F., Lu, X., Wang, T., Wang, Y., Zhang, Z., & Yan, Y. (2013). Triton X-100 directed synthesis of mesoporous γ-Al_2O_3 from coal-series kaolin. *Applied Clay Science*, 85, 31-38.

Pan, F., Lu, X., Wang, T., Wang, Y., Zhang, Z., Yan, Y., et al. (2013). Synthesis of large-mesoporous γ-Al_2O_3 from coal-series kaolin at room temperature. *Materials Letters*, 91, 136-138.

Parry, E. P. (1963). An infrared study of pyridine adsorbed on acidic solids. Characterization of surface acidity. *Journal of Catalysis*, 2(5), 371-379.

Petushkov, A., Yoon, S., & Larsen, S. (2011). Synthesis of hierarchical nanocrystalline ZSM-5 with controlled particle size and mesoporosity. *Microporous Mesoporous Materials*, 137, 92–100.

Platon, A., & Thomson, W. (2003). Quantitative Lewis/Brønsted ratios using DRIFTS. *Applied Catalysis in Industrial Engineering: Chemical Research*, 42, 5988-5992.

Qoniah, I., Prasetyoko, D., Bahruji, H., Triwahyono, S., Jalil, A. A., Suprapto, et al. (2015). Direct synthesis of mesoporous aluminosilicates from Indonesian Kaolin clay without calcination. *Applied Clay Science*, 118, 290–294.

Ramdhani, E. P., Suprapto, Prasetyoko, D., & Hartati. (2018). Synthesis of mesoporous alumina from red mud. *Indonesian Journal of Chemistry. in press.*

Rousseaux, J. M., Weisbecker, P., Muhr, H., & Plasari, E. (2002). Aging of precipitated amorphous alumina gel. *Industrial & Engineering Chemistry Research*, 41(24), 6059-6069.

Snars, K., Gilkes, R., & Wong, M. (2004). The liming effect of bauxite processing residue (red mud) on sandy soils. *Soil Research*, 42 (3), 321–328.

Sushil, S., & Batra, V. S. (2012). Modification of red mud by acid treatment and its application for CO removal. *Journal of Hazardous Materials*, 203, 264-273.

Wang, C.C., & Ying, J.Y. (1999). Sol-gel synthesis and hydrothermal processing of anastase and rutile titania nanocrystals. *Chemistry of Materials*, 11(11), 3113-3120.

Xia, Y., Yang, P., Sun, Y., Wu, Y., Mayers, B., & Gates, B. (2003). One-dimensional nanostructures synthesis, characterization, and applications. *Advance Materials*, 15, 353–390.

Yue, M. B., Jiao, W. Q., Wang, Y. M., & He, M. Y. (2010). CTAB-directed synthesis of mesoporous γ-alumina promoted by hydroxy polyacids. *Microporous and Mesoporous Materials*, 132, 226–231.